1. M.N. Brahami[1,5], 2. I.S. Bousmaha[2,5], 3. S. Boudjella[3], 4. FZ. Boudjella[4], 5. M. Brahami[1,5], 6. S.E. Bechekir[1,5], 7. Khelifi El Mabrouk[1,5]

Djillali Liabes University of Sidi Bel Abbes, Algeria (1), ESSA-Tlemcen, Ecole Supérieure en Sciences Appliquées de Tlemcen, ESSA-Tlemcen. BP 165 RP Bel Horizon, Tlemcen 13000, Algerie (2) University of Mascara, Algeria (3), University of Ain Temouchent, Algeria (4), ICEPS Laboratory, Djillali Liabes University of Sidi-Bel-Abbes, Algeria. (5)

doi:10.15199/48.2024.08.37

A new multilevel inverter topology, controlled by the pulse width and height modulation (PWHM) technique, with a reduced number of switches

Abstract. *Energy harvesting from renewable energy sources is trending in the world due to inventions in modern technology. The electricity generation through a grid-connected PV (photovoltaic) system is of great interest to developing countries. PV systems generate electricity in the form of direct current, while most loads use alternating voltage. Therefore, DC-AC (direct current- alternative current) converters are necessary to supply loads with alternating current and to be able to feed the produced energy into the electrical grid. Indeed, the presence of current or voltage harmonics leads to disturbances in electrical networks. The most well-known adverse effects of harmonic pollution include malfunctions in certain electrical equipment, conductor heating, interference with telecommunication networks, and resonance phenomena with elements composing the network. Improving the performance of a photovoltaic system relies on choosing appropriate control strategies and inverter topologies. Purpose. The objective of this article is to study and implement a static converter (DC-AC) for photovoltaic systems, ensuring efficient adaptation between the energy source and consumers. Novelty. A new multilevel inverter topology with a reduced number of switches is proposed in this article. Method. The inverter is controlled by pulse width and height modulation technique to enhance the quality of the extracted energy and optimize total harmonic distortion (THD) by eliminating low-order harmonics close to the fundamental frequency, while reducing switching losses. Practical value. A detailed study of the proposed new topology (Figure 1), as well as a Fourier series decomposition of the output waveform obtained from the multilevel inverter (Equations 1-28), has been presented to improve the quality of the energy injected into the grid. Simulation results have demonstrated the effectiveness of the employed method (Figures 4-7). A comparison of the proposed topology is made with other conventional inverter topologies in terms of component requirements (Table 1). This comparison highlights the advantage of the proposed topology in terms of component count, particularly for a higher number of voltage levels.*

Streszczenie. *Pozyskiwanie energii ze źródeł odnawialnych jest trendem na świecie ze względu na wynalazki w nowoczesnej technologii. Generowanie energii elektrycznej za pośrednictwem podłączonego do sieci systemu PV (fotowoltaicznego) jest bardzo interesujące dla krajów rozwijających się. Systemy PV wytwarzają energię elektryczną w postaci prądu stałego, podczas gdy większość obciążeń wykorzystuje napięcie przemienne. Dlatego konwertery DC-AC (prąd stały-prąd alternatywny) są niezbędne do zasilania obciążeń prądem przemiennym i do przekazywania wytworzonej energii do sieci elektrycznej. Rzeczywiście, obecność harmonicznych prądu lub napięcia prowadzi do zakłóceń w sieciach elektrycznych. Najbardziej znane negatywne skutki zanieczyszczenia harmonicznymi obejmują awarie niektórych urządzeń elektrycznych, nagrzewanie się przewodów, zakłócenia w sieciach telekomunikacyjnych i zjawiska rezonansu z elementami tworzącymi sieć. Poprawa wydajności systemu fotowoltaicznego polega na wyborze odpowiednich strategii sterowania i topologii falowników. Cel. Celem tego artykułu jest zbadanie i wdrożenie konwertera statycznego (DC-AC) dla systemów fotowoltaicznych, zapewniającego skuteczną adaptację między źródłem energii a odbiorcami. Nowość. W tym artykule zaproponowano nową topologię falownika wielopoziomowego ze zmniejszoną liczbą przełączników. Metoda. Falownik jest sterowany techniką modulacji szerokości i wysokości impulsu w celu zwiększenia jakości wyodrębnionej energii i zoptymalizowania całkowitych zniekształceń harmonicznych (THD) poprzez wyeliminowanie harmonicznych niskiego rzędu zbliżonych do częstotliwości podstawowej, przy jednoczesnym zmniejszeniu strat przełączania. Wartość praktyczna. Przedstawiono szczegółowe badanie proponowanej nowej topologii (rysunek 1), a także rozkład szeregu Fouriera przebiegu wyjściowego uzyskanego z falownika wielopoziomowego (równania 1-28), aby poprawić jakość energii wstrzykiwanej do sieci. Wyniki symulacji wykazały skuteczność zastosowanej metody (rysunki 4-7). Dokonano porównania proponowanej topologii z innymi konwencjonalnymi topologiami falowników pod względem wymagań dotyczących komponentów (tabela 1). Porównanie to podkreśla zaletę proponowanej topologii pod względem liczby komponentów, szczególnie w przypadku większej liczby poziomów napięcia.* (***Nowa topologia inwertera wielopoziomowego, sterowana techniką modulacji szerokości i wysokości impulsu (PWHM) ze zmniejszoną liczbą przełączników***)

Keywords*:* Topology; Multilevel Inverters; The Pulse Width And Height Modulation PWHM; Renewable Energy Sources; Microgrids.
Słowa kluczowe: Topologia; Falowniki wielopoziomowe; Modulacja szerokości i wysokości impulsu PWHM; Odnawialne źródła energii.

Introduction.

Renewable energy sources have a decisive role in the future, as they form the foundation of future electricity production. Generating electricity through a grid-connected PV system holds great significance for developing countries. However, connecting PV systems to the distribution grid can have some impacts on the electrical networks. PV systems generate electricity in the form of direct current (DC), while most loads require alternating current (AC) voltage. Therefore, DC-AC converters are necessary to supply AC power to loads and enable the injection of generated energy into the electrical grid. [1-3]

The major challenges of DC-AC power converters today focus on increasing efficiency [4-6], improving power quality, and enhancing inverter efficiency by reducing total harmonic distortion (THD) as well as minimizing conduction and switching losses [7]. However, switching losses are higher than conduction losses and are proportional to the number of switching states. Several studies have been conducted to address and mitigate these issues [5-8]. However, all these studies require high switching frequencies, which result in increased switching losses. Thus, for practical implementation, reducing the switching frequency is also essential.

Control techniques that rely on predefined switching angles by decomposing a PWM (pulse wight modulation) signal into a Fourier series exhibit better performance in terms of THD, elimination of low-order harmonics, reduction of switching losses, and control of the peak value of the fundamental component of the output voltage.

For the integration of PV systems into the grid, the use of a conventional two-level inverter produces a square wave that is not suitable for most complex applications. In such cases, a pure sine wave is desired. Furthermore, the rated power of traditional converters is limited by the rated power of the semiconductor devices used and the allowed switching frequencies.

Conventional inverters based on frequency transformers operating at 50 Hz and AC filters are commonly used in renewable energy systems to increase the voltage to grid

voltage levels of 6 to 36 kV and to reduce voltage THD, respectively. The investment and installation costs are high due to their weight and size [8-11].

With the emergence of new high-power semiconductor devices, new power conversion structures are being designed to meet the needs of future medium or high-voltage systems. In this highly active field, the topologies and circuits of cascaded modular multilevel converters (MMC) have attracted significant attention for their application in medium and high-voltage systems [12-15]. The number of components in MMC converters increases linearly with the number of levels. However, the MMC converter requires multiple isolated and balanced DC current sources [16-20].

A new topology of a three-phase multilevel inverter controlled by pulse width and height modulation technique is presented to improve the quality of the energy produced and injected into the grid, optimizing THD by eliminating low-order harmonics close to the fundamental frequency, while reducing switching losses.

The proposed new topology of a three-phase inverter consists of N levels in the output voltage waveform line-to-neutral and can be used to supply a microgrid with ns renewable energy sources (such as photovoltaic, wind, etc.) with optimized THD. It involves a series connection of N conventional two-level inverters (±E, 0) per phase. Each stage of the conventional inverter is powered by a renewable energy source, with a total number of DC sources being ns =N+4. In this paper, a six-level inverter application has been constructed, and the topology is controlled by a pulse width and height modulation technique.

Topology and operating principle of multilevel inverters

Figure 1 shows the topology of a six-level three-phase inverter. It consists of 10 sources of DC voltage, supplying a balanced three-phase load. In general, the DC voltage sources can have different values. However, in order to optimize the total harmonic order of the multi-level output waveform, they are considered to be optimized and controlled.

Operating principle

The required six-phase-neutral output voltage levels *(±E3; ±(E' = E2 + E3); ±EE = E1 + E2 + E3))* are generated as follows:

1) When switches *S1.1, S5.1*, and *S9.1* are activated during the first cycle *[0; α1],* the resulting single-phase voltage will be *V1 = E1 + E2 + E3.*

2) When switches *S1.1, S6.1*, and *S9.1* are activated during the second cycle *[α1; α2],* the resulting single-phase voltage will be *V1 = E2 + E3.*

3) When switches *S2.1, S6.1*, and *S9.1* are activated during the third cycle *[α2; α3],* the resulting single-phase voltage will be *V1 = E3.*

4) When switches *S3.1, S7.1,* and *S10.1* are activated during the fourth cycle *[α3; α4],* the resulting single-phase voltage will be *V1 = -E3.*

5) When switches *S4.1, S7.1,* and *S10.1* are activated during the fifth cycle *[α4; α5],* the resulting single-phase voltage will be *V1 = -(E2 + E3).*

6) When switches *S1.1, S6.1*, and *S9.1* are activated during the sixth cycle *[α5; α6],* the resulting single-phase voltage will be *V1 = -(E1 + E2 + E3).*

Pulse Width and Height Modulation (PWHM) technique

A multilevel converter can produce a symmetric staircase waveform with respect to one-quarter of the period, synthesized by multiple DC voltage sources.

In general, the most significant low-frequency harmonics are chosen to be eliminated by properly selecting the switching angles, and high-frequency harmonic components can be easily filtered out using additional filtering circuits.

To optimize the THD of the proposed inverter's phase-neutral output voltage waveform, the Pulse Width and Height Modulation (PWHM) technique is employed. The heights (amplitudes *E1, E2, E3*) and widths (angles *α1, α2*) of the output waveform are calculated to cancel out the maximum number of harmonics and optimize the THD. [21,22]

Figure 2 shows the staircase-like output voltage signal of the six-level inverter.

The duration of each step depends on its conduction angle *α1, α2, ...,* which is determined based on the eliminated harmonic component.

The method for calculating the unknown angles utilizes the interval *[0; π/3]* for a three-phase approach.

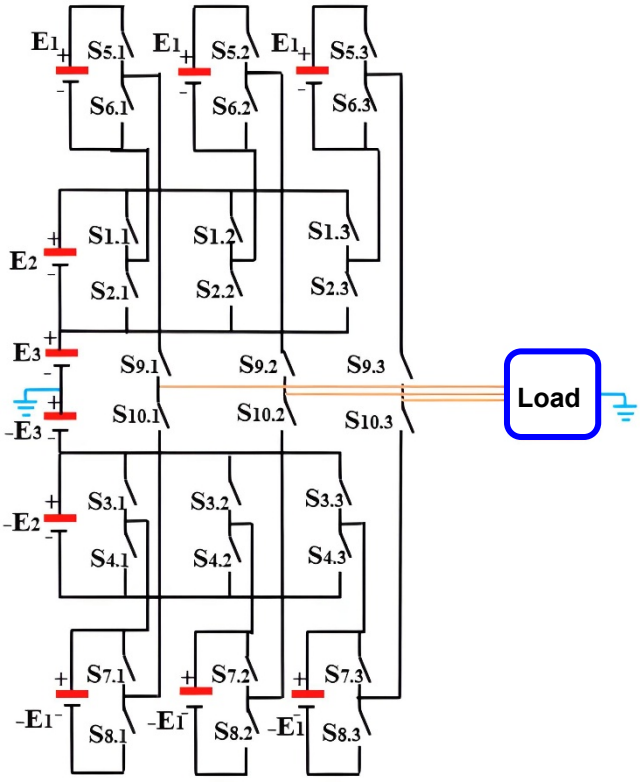

Fig.1. Proposed six-level voltage inverter topology.

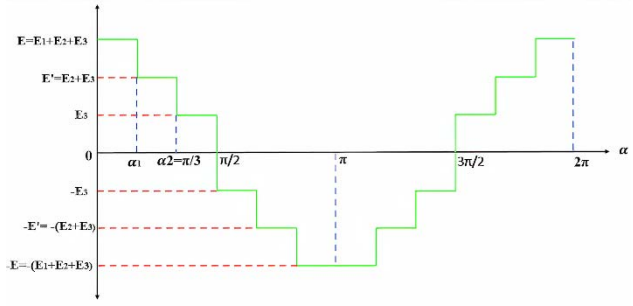

Fig. 2. Phase-neutral output voltage waveform of the six-level inverter.

Decomposition of a signal into a Fourier series

Any periodic signal, including the output voltage of the multilevel inverter using the fundamental switching frequency, can be expressed using the Fourier series decomposition:

(1) $v(t) = a_0 + \sum_{n=1}^{\infty} [a_n \cos(n\omega t) + b_n \sin(n\omega t)]$

Où a_0, a_n et b_n are the Fourier coefficients.

(2) $$\begin{cases} a_0 = \frac{1}{T}\int_0^T u(t)d\omega t \\ a_n = \frac{1}{T}\int_0^T u(t)\cos(n\omega t)d\omega t \\ b_n = \frac{1}{T}\int_0^T u(t)\cos(n\omega t)d\omega t \end{cases}$$

Where T is the fundamental period of *u(T)*.

To simplify the Fourier series, various symmetries will be considered: odd sinusoidal symmetry, half-wave symmetry, and odd quarter-wave symmetry.

The values of *a1, a2*, and *E1, E2, E3* can be chosen to eliminate low-frequency harmonics or to achieve minimum total harmonic distortion (THD).

In a three-phase approach, there are several properties that can reduce the time interval required to find a solution for the set of equations below. Thus, instead of searching in the interval $(0, \pi/2)$, it will be $(0, \pi/3)$.

The calculation steps are presented as follows.

We list the properties and characteristics of the ideal voltage waveform of the three balanced voltages [23-25]:

1. Property (1): is an even function with respect to zero.

For each $\alpha \in \left[0, \frac{\pi}{2}\right]$, $v_a(-\alpha) = v_a(\alpha)$

2. Property (2): *Va* is an odd function with respect to $\pi/2$.

For each $\alpha \in \left[0, \frac{\pi}{2}\right]$, $v_a(\frac{\pi}{2}+\alpha) = -v_a(\frac{\pi}{2}-\alpha)$

3. Property (3): *Vb* is symmetric to *Va* with respect to $\pi/3$.

For each $\alpha \in \left[0, \frac{\pi}{3}\right]$, $v_b(\frac{\pi}{3}+\alpha) = -v_a(\frac{\pi}{3}-\alpha)$

4. Property (4): *Vc* is a reversed and shifted signal of *Va*.

For each $\alpha \in \left[0, \frac{\pi}{3}\right]$, $v_c(\frac{\pi}{3}+\alpha) = -v_a(\alpha)$

5. Property (5): *Va*, *Vb* and *Vc* are balanced three-phase voltages.

For each $\alpha \in [0, 2\pi]$, $v_a(\alpha) + v_b(\alpha) + v_c(\alpha) = 0$

The above properties of the ideal voltage waveform of the three balanced voltages are attributed to the output voltage waveform of the inverter, focusing on the range *(0, π/3)*. The Fourier coefficients of the phase-neutral output voltage, given by (3), are also used because it is well known that every periodic function can be composed of a set of sinusoidal functions [22]:

(3) $$\begin{cases} a_n = \frac{1}{\pi}\int_{-\pi}^{\pi} v_a(\alpha)\cos(n\alpha)d\alpha \\ b_n = \frac{1}{\pi}\int_{-\pi}^{\pi} v_a(\alpha)\sin(n\alpha)d\alpha \end{cases}$$

Applying property (1) to the Fourier coefficients, we obtain:

(4) $$\begin{cases} a_n = \frac{2}{\pi}\int_0^{\pi} v_a(\alpha)\cos(n\alpha)d\alpha \\ b_n = 0 \end{cases}$$

(5) $a_n = 0$ For even n,

(6) $a_n = \frac{4}{\pi}\int_0^{\pi/2} v_a(\alpha)\cos(n\alpha)d\alpha$ For odd n,

Applying property (5) to the Fourier coefficients, we obtain:

(7)

$$a_n = \frac{4}{\pi}\left[\int_0^{\pi/3} v_a(\alpha)\cos(n\alpha)d\alpha - \int_{\pi/3}^{\pi/2}(v_b(\alpha)+v_c(\alpha))\cos(n\alpha)d\alpha\right]$$

(8)

$$a_n = \frac{4}{\pi}\left[\int_0^{\pi/3} v_a(\alpha)\cos(n\alpha)d\alpha - \int_{\frac{\pi}{3}}^{\frac{\pi}{2}}\left(v_b(\frac{2\pi}{3}-\alpha)+v_c\left(a-\frac{2\pi}{3}\right)\cos(n\alpha)d\alpha\right]\right.$$

Due to the properties of the mentioned three-phase output voltage, we have [22]:

(9) $$\begin{cases} a_n = \frac{8}{\pi}\cos\left(n\frac{\pi}{6}\right)\int_0^{\pi/3} v(\alpha)\cos\left(n\left(\frac{\pi}{6}+\alpha\right)\right)d\alpha \\ b_n = 0 \end{cases}$$

Where *n* is an odd and non-triple harmonic, and *v* is the line-to-neutral voltage.

The three phase voltages *(Va, Vb, Vc)* are assumed to have the same symmetric properties as an ideal three-phase voltage system. The asymmetric properties with respect to to $\frac{\pi}{2}v_a(\frac{\pi}{2}+\alpha) = -v_a(\frac{\pi}{2}+\alpha)$, allow for the cancellation of all even-order harmonics. The Fourier coefficients of the phase voltage in the interval *[0, π/3]* can be expressed as follows:

(10) $a_{n=2p+1} = \frac{8}{\pi}\cos\left(n\frac{\pi}{6}\right)\int_0^{\pi/3} v_a(\alpha)\cos\left(n\left(\frac{\pi}{6}+\alpha\right)\right)d\alpha$

Using $n = 3(2p+1)$ We obtain $\cos\left(n\frac{\pi}{6}\right) = \cos\left[(2p+1)\left(\frac{\pi}{2}\right)\right] = 0$. This means that all even harmonics and multiples of three are canceled out.

By utilizing various symmetrical properties, we obtain *a2= π/3*. "The remaining non-cancelled harmonics are of the order 6q±1."

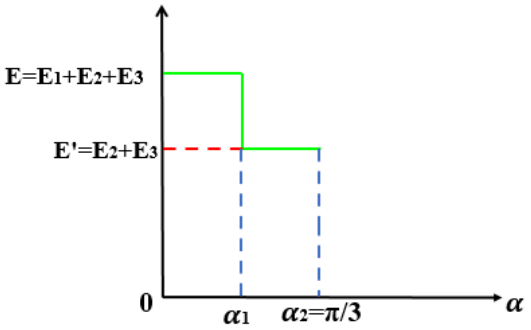

Fig. 3. Waveform of the single-phase voltage Va within [0, π/3].

Equation (10) shows that adjusting the value of *Va* is only possible within the interval *[0, π/3]*. The symmetry property of an ideal three-phase voltage system allows determining the value of *Va* over the interval *[0, 2π]*; Therefore, the following analysis will be limited to the interval [0, π/3].

The single-phase voltage *Va* is assumed to have two DC levels *(E; E')* within the interval *[0, π/3]* as illustrated in Figure 3. *Va* is assumed to have two pulses. The first pulse has a height (amplitude) of *E* and a width (angle) of *a1*. The

second pulse has a height of E' and a $(\pi/3 - a1)$. The heights and widths are defined to cancel out the maximum number of successive harmonics.
By substituting the value of the voltage Va as shown in Figure 3 into Eq. 10, the Fourier coefficients in this case can be written as follows:

$$(11)\quad a_n = \frac{8}{\pi}\cos\left(n\frac{\pi}{6}\right)\int_0^{\pi/3} v_a(\alpha)\cos\left(n\left(\frac{\pi}{6}+\alpha\right)d\alpha\right)$$

(12)

$$a_n = \frac{8}{\pi}\cos\left(n\frac{\pi}{6}\right)\left[\begin{array}{l}\int_0^{a_1} v_a(\alpha)\cos\left(n\left(\frac{\pi}{6}+\alpha\right)d\alpha\right)\\ +\int_{\alpha_1}^{\alpha_2} v_a(\alpha)\cos\left(n\left(\frac{\pi}{6}+\alpha\right)d\alpha\right)\end{array}\right]$$

(13)

$$a_n = \frac{8}{\pi}\cos\left(n\frac{\pi}{6}\right)\left[\begin{array}{l}\frac{E}{n}\left(\sin\left(n\left(\frac{\pi}{6}+\alpha_1\right)\right)-\sin\left(n\frac{\pi}{6}\right)\right)\\ +\frac{E'}{n}\left(\sin\left(n\left(\frac{\pi}{6}+\alpha_2\right)\right)-\sin\left(n\frac{\pi}{6}+\alpha_1\right)\right)\end{array}\right]$$

With: $\alpha_2 = \frac{\pi}{3}$

$$(14)\quad \frac{a_n}{E} = \frac{8}{n\pi}\cos\left(n\frac{\pi}{6}\right)\left[\begin{array}{l}\sin\left(n\left(\frac{\pi}{6}+\alpha_1\right)\right)-\sin\left(n\frac{\pi}{6}\right)\\ +\frac{E'}{E}\left(\sin\left(n\left(\frac{\pi}{6}+\frac{\pi}{3}\right)\right)-\sin\left(n\left(\frac{\pi}{6}+\alpha_1\right)\right)\right)\end{array}\right]$$

Let us define :

$$(15)\quad r = \frac{E'}{E}$$

$$(16)\quad \frac{a_n}{E} = \frac{8}{n\pi}\cos\left(n\frac{\pi}{6}\right)\left[\begin{array}{l}\sin\left(n\left(\frac{\pi}{6}+\alpha_1\right)\right)-\sin\left(n\frac{\pi}{6}\right)\\ +r.\sin\left(n\left(\frac{\pi}{6}+\frac{\pi}{3}\right)\right)-r.\sin\left(n\frac{\pi}{6}+\alpha_1\right)\end{array}\right]$$

$$(17)\quad \frac{a_{n=6q\pm1}}{E} = \frac{8}{n\pi}\cos\left(n\frac{\pi}{6}\right)\left[\begin{array}{l}(1-r)\sin\left(n\left(\frac{\pi}{6}+\alpha_1\right)\right)\\ +r.\sin\left(n\left(\frac{\pi}{6}+\frac{\pi}{3}\right)\right)-\sin\left(n\frac{\pi}{6_1}\right)\end{array}\right]$$

r is the ratio of the two DC voltage levels, and $a1$ is the switching angle from E to E'. $\alpha 1$ and r represent the two adjustable variables available.

Harmonic Elimination Technique

The selected harmonics can be eliminated through an appropriate selection of the adjustable variables $a1$ and r. The system of nonlinear equations (see Eq. 17) can only be mathematically solved if the number of equations matches the number of unknown variables. Since only two adjustable variables are available, only two harmonics from Eq. 4 can be obtained. It is well-known that low-order harmonics are more harmful than higher-order harmonics. Spectral analysis reveals that among the lower-order harmonics (below 10), only the 5th and 7th order harmonics are not cancelled out. They can be eliminated only if condition (18) is satisfied.

$$(18)\quad \begin{cases}\frac{a_5}{E} = 0\\ \frac{a_7}{E} = 0\end{cases}$$

In this case, the first non-zero harmonic is the 11th harmonic, where $n \in \{1, 11, 13, 17, 19, \ldots 6q \pm 1\}$. By combining (17) and (18), we obtain a nonlinear system of two equations with two unknowns $(a1, r)$.

$$(19)\quad \begin{cases}(1-r)\sin\left(5a_1+5\frac{\pi}{6}\right)+r.\sin\left(5\frac{\pi}{3}+5\frac{\pi}{6}\right)=+\frac{1}{2}\\ (1-r)\sin\left(7a_1-\frac{\pi}{6}\right)+r.\sin\left(7\frac{\pi}{3}-\frac{\pi}{6}\right)=-\frac{1}{2}\end{cases}$$

By solving (19) using the bisection method within the interval $[0, \pi/3]$, the values of $a1$ and r are:

$$(20)\quad \alpha_1 = \frac{\pi}{6}$$

$$r = \sqrt{3} - 1$$

Therefore

$$(21)\quad \begin{cases}\frac{a_1}{E} = \frac{12}{\pi}(2-\sqrt{3}) = 1.0235\\ a_{(n=12\ p-1)} = -\frac{a_1}{n}\\ a_{(n=12\ p+1)} = \frac{a_1}{n}\\ a_n = 0\ if\ \rightarrow\ n \neq 12\ p \pm 1\end{cases}$$

Using the symmetry properties of an ideal three-phase system, the output voltages are reconstructed within the interval $(\pi/2, \pi/3)$.
Therefore, a third voltage level $E3$ appears within the interval $(\pi/2, \pi/3)$.
With:

$$(22)\quad E = E_1 + E_2 + E_3$$

$$(23)\quad E' = E_2 + E_3$$

$$(24)\quad r = \frac{E'}{E}$$

Let's define:

$$(25)\quad E = 1pu,\ E' = r.E = \left(\sqrt{3}\right)$$

$$(26)\quad E' = r.E = \left(\sqrt{3}-1\right).1pu = 0.732pu$$

$$(27)\quad E_1 = E_3 = E - E' = 1pu - 0.732pu = 0.268pu$$

$$(28)\quad E_2 = E' - E_3 = 0.732 - 0.268 = 0.464pu$$

Simulation and Interpretation of Results

To better evaluate the performance of the proposed topology, two simulation scenarios are considered. The different parameters are as follows:

$$E = E_1 + E_2 + E_3 = 100V$$

$$E' = r.E = \left(\sqrt{3}-1\right).100 = 73.2V$$

$$E_1 = E_3 = E - E' = 100 - 73.2 = 26.8V$$

$$E_2 = E' - E_3 = 73.2 - 26.8 = 46.4V$$

The scenarios involve supplying a resistive, inductive, and star-connected load.

1) Scenario 1: Pure resistive load connected in star configuration (R = 45Ω):
In this scenario, the resistive load is connected in a star configuration. The line current has the same waveform as the phase-to-neutral voltage due to the resistive nature of the load, as shown in Figure (4 and 5). The THD (Total Harmonic Distortion) value of the current/voltage is 15.21%, and the fundamental amplitude of the voltage is 106.4V, while the current is 2.365A.

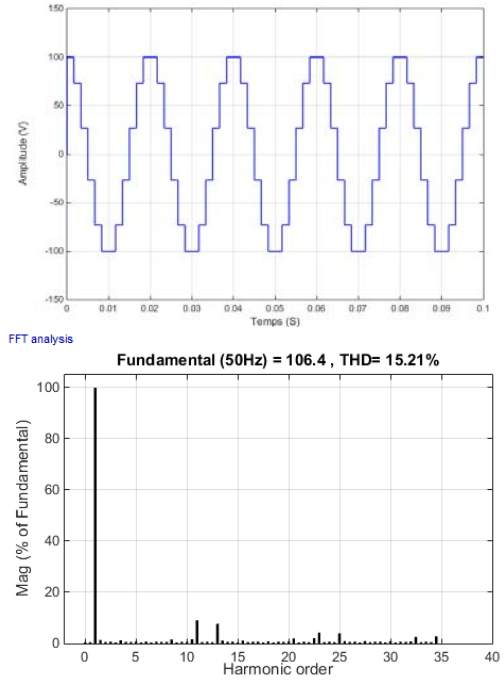

Fig.4. Waveform of the Output Voltage and its Harmonic Spectrum

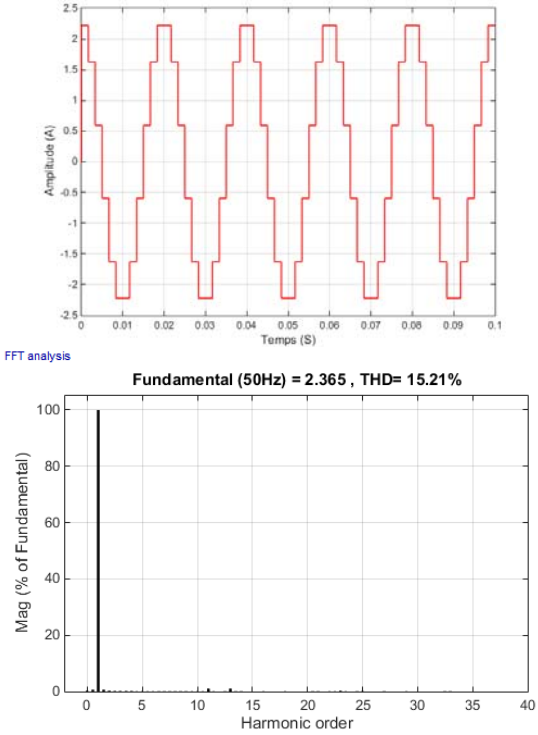

Fig. 5. Waveform of the Output Current and its Harmonic Spectrum

2) Scenario 2: Inductive load connected in star configuration (R = 45Ω, L = 245mH):
In this case, we consider an inductive load connected in a star configuration. The current waveform and its spectrum show that there are almost no harmonics present (Figure 7). The THD value in this case is also very low, at 1.32%, and the first non-zero harmonic is the 11th harmonic with an amplitude of 1.03%. The main reason for the very low THD value is the inductive load, which behaves like a low-pass filter.
The waveform of the voltage and its harmonic spectrum show a THD of 15.11% and a fundamental amplitude of 102.7V. The first non-zero harmonic is the 11th harmonic with a rate of 8.72%.

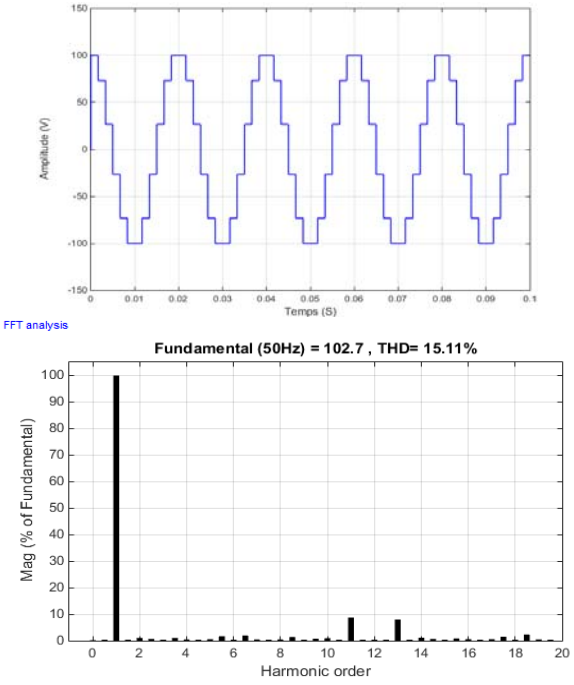

Fig. 6. Waveform of the Output Voltage and its Harmonic Spectrum

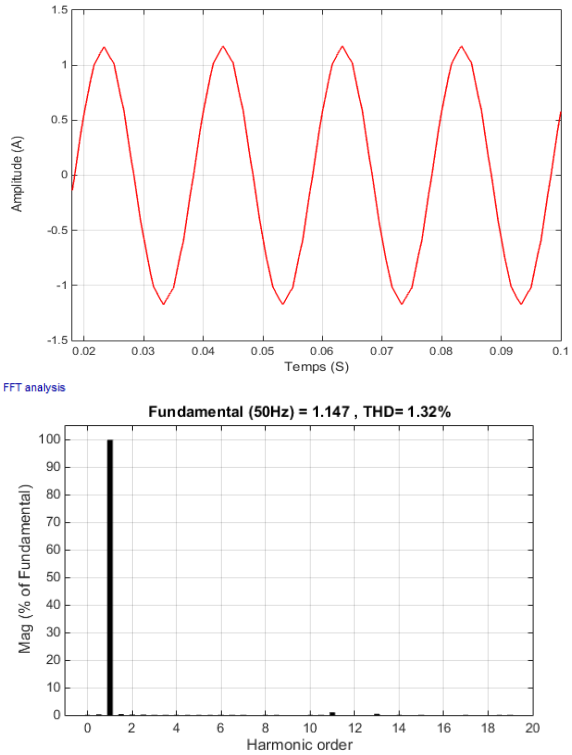

Fig. 7. Waveform of the Output Current and its Harmonic Spectrum

The simulation results demonstrate the effectiveness of the proposed harmonic elimination technique (i.e., selection of $a1$ and r). Figures 5 and 7 (Fast Fourier Transform "FFT" analysis) also show the elimination of the first harmonics in the line currents for both different scenarios. The FFT

analysis for the voltage shows the elimination of the 5th and 7th harmonics. The first non-zero harmonic is the 11th order. The FFT analysis also reveals very low THD values for both the current and voltage, compared to previous control techniques.

Comparison with Other Topologies

In this section, a comparison of the proposed topology is made with other conventional inverter topologies in terms of component requirements.

Table 1. Number of Components and DC Sources for Different Inverter Topologies

Topology	NPC (Neutral point clamped)	FC (Flying Capacitor)	CHB (Cascaded H-Bridge)	**Proposed Topology**
Number of DC Sources	(N-1)	(N-1)	3(N - 1) /2	N+4
Number of Power Transistors	6(N-1)	6(N-1)	6(N-1)	6(N-1)
Number of Diodes	6(N-1)	6(N-1)	6(N-1)	6(N-1)
Number of Freewheeling Diodes	3(N -1) (N - 2)	0	0	0
Number of Capacitor	0	(3/2)(N - 1) (N -2)	0	0

The component requirements of the different topologies for a three-phase configuration are indicated in Table .1 in terms of the number of voltage levels (N) in the single-phase voltage. From this table, we can deduce that the number of components in the proposed structure is lower than that of the other topologies, especially for a higher number of voltage levels.

A comparison is made with the CHB (Cascaded H-Bridge) topology because, as mentioned earlier, the proposed topology resembles the CHB in terms of configuration and functional characteristics. For example, implementing a 35-level voltage inverter would result in 51 sources for the CHB topology, but only 39 sources for the proposed topology.

This comparison highlights the advantage of the proposed topology in terms of component count, particularly for higher numbers of voltage levels.

Inmterpretation

Achieving low THD and increasing the number of eliminated lower-order harmonics in conventional two-level inverters requires a high switching frequency, which results in significant switching losses.

The proposed topology only uses 12 switching states per period and enables the elimination of harmonics from the 2nd to the 10th order without the need for additional filtering circuits. This approach allows for a substantial reduction in the switching frequency compared to traditional topologies.

By reducing the switching frequency, the proposed topology offers several benefits. First, it reduces the switching losses, leading to improved efficiency. Second, it decreases the stress on the power electronic components, prolonging their lifespan. Third, it simplifies the design and control of the inverter system.

Overall, the proposed topology provides a more efficient and reliable solution for harmonic elimination, addressing the limitations of conventional two-level inverters and offering advantages in terms of performance and component count.

Conclusion

The proposed multi-level inverter topology can be a good solution for powering a microgrid from renewable energy sources. A six-level inverter was considered and controlled using the PWHM technique, requiring only twelve switching states per period. The simulation results showed a voltage THD rate of 15%, with successive harmonics being zeroed from the 2nd to the 10th order. The first non-zero harmonic is the 11th order with 8% of the fundamental amplitude.

The proposed configuration provides a compact and cost-effective system with a reduced number of switching states. The low-frequency switching reduces the power losses of the inverter, resulting in improved efficiency of the proposed topology. Additionally, the proposed topology significantly reduces the number of components required for the same number of voltage levels compared to conventional topologies.

Overall, the proposed multi-level inverter topology offers advantages in terms of harmonic performance, compactness, cost-effectiveness, and reduced switching losses. It provides a viable solution for integrating renewable energy sources into microgrids.

REFERENCES

[1] BRAHAMI, Mohammed Nadjib, BOUDJELLA, Fatima Zohra, NEMMICH, Said, et al. IDENTIFYING OPTIMAL ORIENTATION OF A PHOTOVOLTAIC GENERATOR FOR OZONE WATER TREATMENT. Environmental Engineering & Management Journal (EEMJ), (2020). vol. 19, no 12.

[2] MAKA, Ali OM et ALABID, Jamal M. Solar energy technology and its roles in sustainable development. Clean Energy, (2022). vol. 6, no 3, p. 476-483. DOI:

[3] MOHAMMED, Laith A., HUSSEIN, Taha A., et SADOON, Ahmed T. High performance of multilevel inverter reduced switches for a photovoltaic system. *Przeglad Elektrotechniczny*, 2022, vol. 98, no 8

[4] DESHPANDE, Soham et BHASME, N. R. A review of topologies of inverter for grid connected PV systems. Innovations in Power and Advanced Computing Technologies (i-PACT). IEEE, (2017). p. 1-6.

[5] BOEH, Magnus, LOHNER, Andreas, et EL AMRANI, Noureddine. (2017). Efficiency increasing by a variable DC link voltage in combination with a bang-bang controlled inverter for an automotive application. In: PCIM Europe; International Exhibition and Conference for Power Electronics, Intelligent Motion, Renewable Energy and Energy Management. VDE2017, p. 1

[6] BOUDJELLA, Fatima Zohra, BOUKLI HACÈNE, Fouad, BOUCHAKOUR, Abdelhak, et al. Simulation and realisation of a three-phase inverter controlled through sinus triangle and space vector pulse width modulation for photovoltaic systems. International Journal of Ambient Energy (2020) , vol. 43, no 1, p. 2360-2368.

[7] FERNÁNDEZ, Efrén, PAREDES, Alejandro, SALA, Vicent, et al. A simple method for reducing THD and improving the efficiency in CSI topology based on SiC power devices. Energies, (2018). vol. 11, no 10, p. 2798.

[8] KARPE, Suraj Rajesh, DEOKAR, Sanjay A., et DIXIT, Arati M. Switching losses minimization and performance improvement of PCC and PTC methods of model predictive direct torque control drives with 15-level inverter. Journal of Electrical Systems and Information Technology, (2018). vol. 5, no 3, p. 759-776.

[9] Boudjella Fatima Zohra, Bousmaha IS, Bechekir S, Brahami M, Ould Abdesslam D, Contribution of the selective harmonic elimination control to the improvement of the output wave quality of a two-level inverter dedicated to renewable energies. Conférence Internationale sur les sciences et génie des atériaux et leurs impacts sur l'environnement ICMSE-19, Sidi Bel Abbès. (2019).

[10] AHMED, Sajjad, SAQIB, Muhammad Asghar, KASHIF, Syed Abdul Rahman, et al . A Modified Multi-Level Inverter System for Grid-Tied DES Applications. Sustainability, (2022). vol. 14, no 24, p. 16545.

[11] MEHTA, Shivinder et PURI, Vinod. A review of different multi-level inverter topologies for grid integration of solar photovoltaic system. Renewable Energy Focus. (2022).
[12] SURESH, K. et PARIMALASUNDAR, E. A modified multilevel inverter with inverted SPWM control. IEEE Canadian Journal of Electrical and Computer Engineering, (2022) vol. 45, no 2, p. 99-104.
[13] BOUSMAHA, Imen Souhila, BECHEKIR, Seyf Eddine, , Djaffar Ould Abdesslam et al. . SHEPWM in three-phase voltage source inverters by modified Newton–Raphson. International Journal of Power Electronics and Drive Systems, (2023), vol. 14, no 1, p. 25.
[14] DURGALAKSHMI, K., ANBARASU, P., KARPAGAM, V., et al. .Utilization Of Reduced Switch Components With Different Topologies In Multi-Level Inverter For Renewable Energy Applications-A Detailed Review. In : 2022 5th International Conference on Contemporary Computing and Informatics (IC3I). (2022) IEEE. p. 913-920.
[15] SOLAS, Estibaliz, ABAD, Gonzalo, BARRENA, Jon Andoni, et al.. Modular multilevel converter with different submodule concepts Part I: Capacitor voltage balancing method. IEEE Transactions on Industrial Electronics, (2012) vol. 60, no 10, p. 4525-4535.
[16] SHI, Xiaojie, LIU, Bo, WANG, Zhiqiang, et al. Modeling, control design, and analysis of a startup scheme for modular multilevel converters. IEEE Transactions on Industrial Electronics, (2015). vol. 62, no 11, p. 7009-7024.
[17] LI, Rui, FLETCHER, John E., XU, Lie, et al. A hybrid modular multilevel converter with novel three-level cells for DC fault blocking capability. IEEE Transactions on Power Delivery, (2015). vol. 30, no 4, p. 2017-2026
[18] LAKSHMI, G. Sree, SREESHOBHA, E., et KUMAR, S. Naveen. Comparison of Multilevel Inverters with T-type Inverter. *Przeglad Elektrotechniczny*, 2023, vol. 99, no 6.
[19] *PARIMALASUNDAR, Ezhilvannan, KUMAR, Nathella Munirathnam Giri, GEETHA, Prahalathan, et al. Performance investigation of modular multilevel inverter topologies for photovoltaic applications with minimal switches. (2022).*
[20] DENG, Fujin et CHEN, Zhe. A control method for voltage balancing in modular multilevel converters. IEEE Transactions on Power Electronics, (2013). vol. 29, no 1, p. 66-76.
[21] CHAVAN, Prakash, PATIL, Akash, PATIL, Suraj, et al. Smart Grid Integration: Renewable Based Micro Hybrid Power System. Asian Journal For Convergence In Technology (AJCT). (2019).
[22] AMAMRA, Sid-Ali, MEGHRICHE, Kamal, CHERIFI, Abderrezzak, et al. Multilevel inverter topology for renewable energy grid integration. IEEE Transactions on Industrial Electronics, (2016). vol. 64, no 11, p. 8855-8866.
[23] MANSOURI, O., ALLAH, M. Khair, MEGHRICHE, K., et al. Three-phase static inverter using a novel precalculated switching method. In : IECON 2007-33rd Annual Conference of the IEEE Industrial Electronics Society. (2007). IEEE. p. 1530-1535.
[24] JARJES, Muhammed K. et HUSSEIN, Taha A. Comparative study of SPWM and SVPWM techniques for the control of three-phase grid connected inverter. *Przeglad Elektrotechniczny*, 2023, vol. 99, no 5.
[25] ABED, Adnan Majeed, ALKHAZRAJI, Afaneen Anwer, et ABDULLA, Shatha S. Active and reactive power control in a three-phase Photovoltaic inverter. *Przeglad Elektrotechniczny*, 2023, vol. 99, no 4